Supporting Information for

Ru Nanocrystals with Shape-Dependent SERS and Catalytic Properties: Controlled Synthesis and DFT Calculations

An-Xiang Yin,[‡] Wen-Chi Liu,[‡] Jun Ke, Wei Zhu, Jun Gu, Ya-Wen Zhang* and Chun-Hua Yan*

Beijing National Laboratory for Molecular Sciences, State Key Laboratory of Rare Earth Materials Chemistry and Applications, PKU-HKU Joint Laboratory in Rare Earth Materials and Bioinorganic Chemistry, College of Chemistry and Molecular Engineering, Peking University, Beijing 100871, China

Supplementary Data

Table S1. Calculated adsorption energies of possible reaction intermediates on $Ru(10\text{-}10)_a$, $Ru(10\text{-}10)_b$ and Ru(0001).

	$Ru(10\text{-}10)_a$ (eV)	$Ru(10\text{-}10)_b$ (eV)	Ru(0001) (eV)
CO	-2.04	-2.08	-1.88
HCHO	-0.68	-0.60	-0.32
H_2CO_3	-0.72	-0.46	-0.18
$H_2C_2O_4$	-1.60	-1.19	-0.22

Table S2. Edge-length and thickness of the Ru nanoplates (triangle and irregular) and capped columns, and diameter of the Ru nanospheres.

	Edge-length (nm)	Thickness (nm)	Diameter (nm)
Triangle nanoplates	23.8 ± 4.6	3.0 ± 0.6	--
Irregular nanoplates	15.1 ± 2.7 [a]	1.5 ± 0.2	--
Capped columns	--	~ 20	~ 75 [b]
Capped columns with elongated trunk	--	~ 45	~ 90 [b]
Nanospheres	--	--	3.0 ± 0.3

[a] The edge-length of irregular nanoplates is the longest diagonal length. [b] The diameter of capped columns (with and without elongated trunk) is the longest diagonal length of their ending plates.

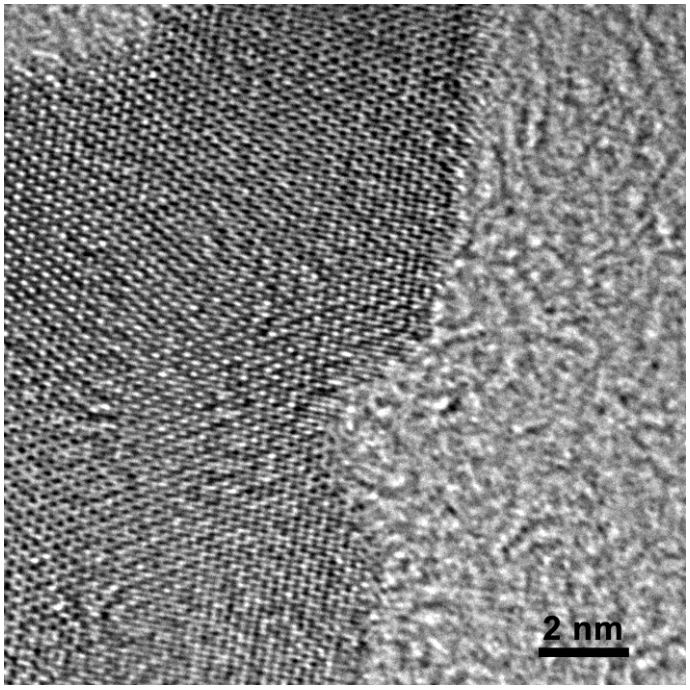

Figure S1. HRTEM image of the edge section of a single Ru triangle nanoplate.

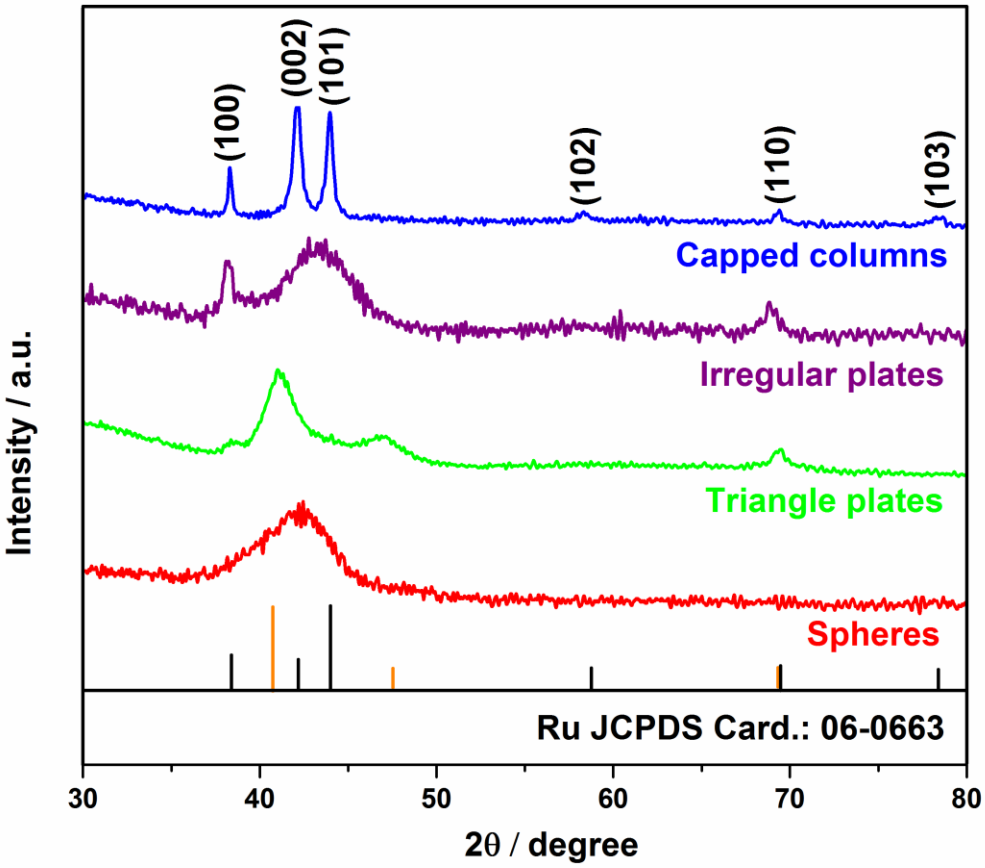

Figure S2. XRD patterns of the as-prepared Ru nanoplates, nanospheres and capped columns. The calculated XRD pattern of *fcc* Ru is shown in orange color (see Ref. S1).

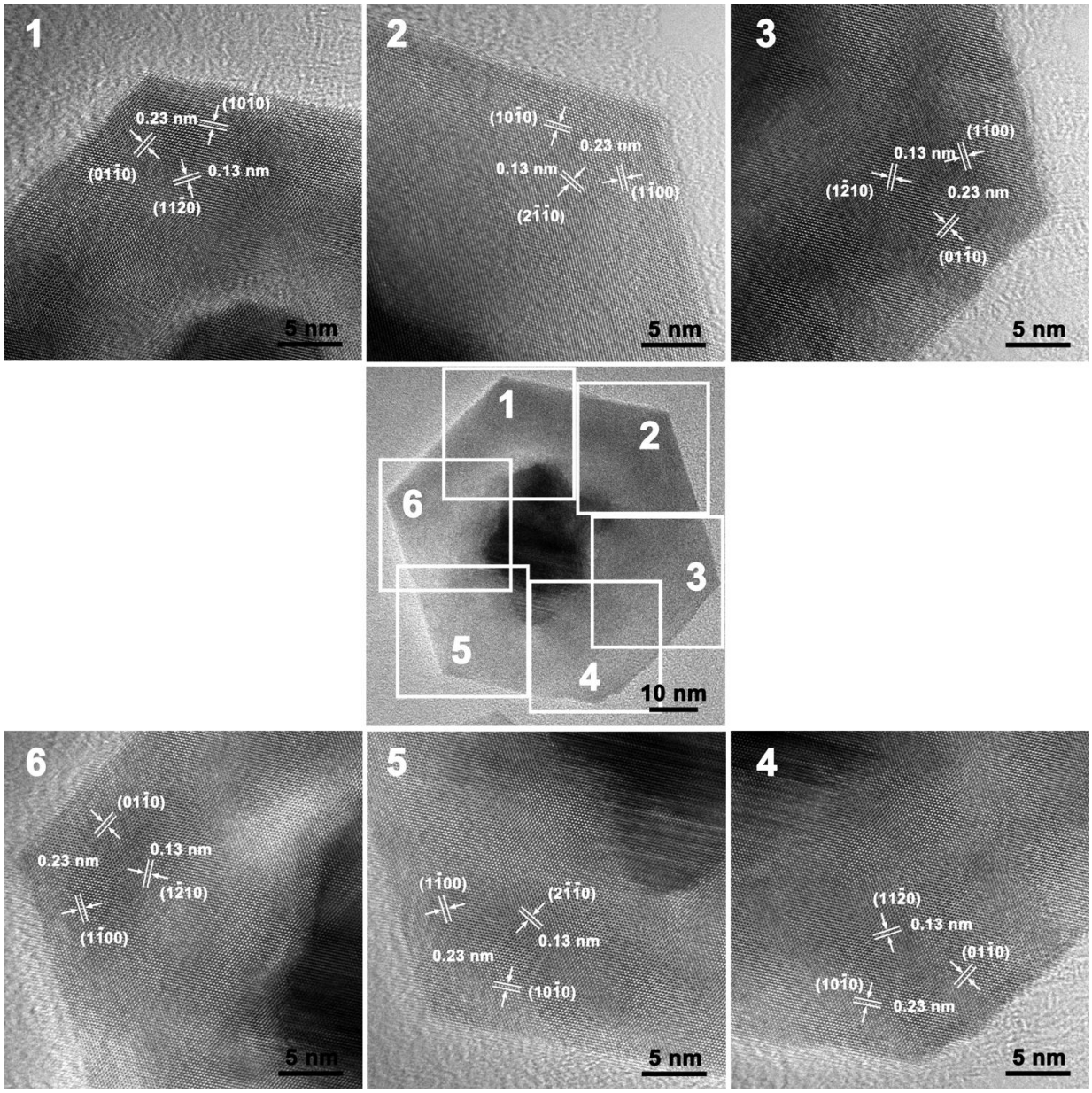

Figure S3. HRTEM images of a single as-prepared Ru capped column. Panels 1-6 are HRTEM images with higher magnifications of the corresponding areas in the capped column nanocrystal shown in the central panel.

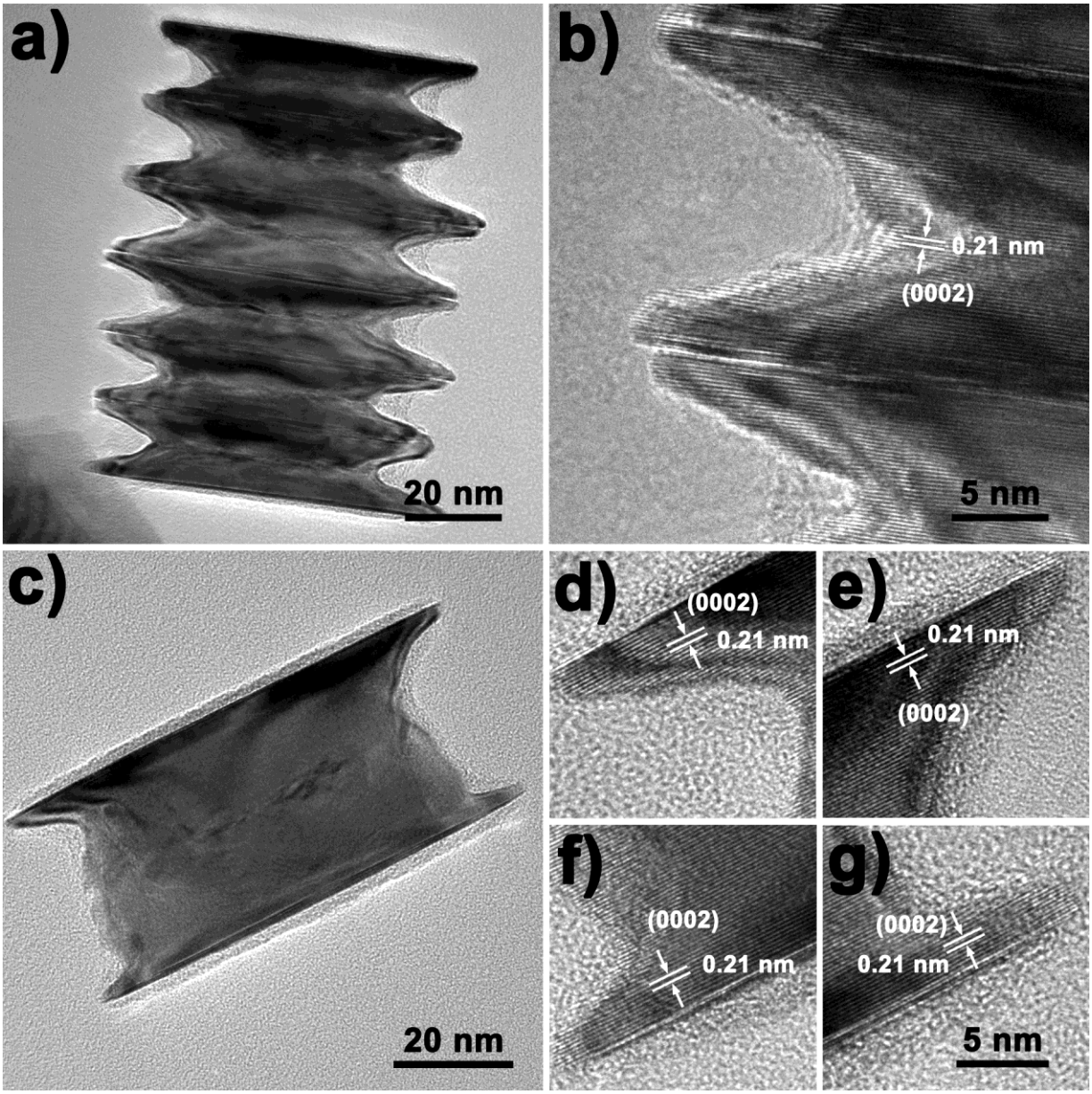

Figure S4. TEM and HRTEM images of Ru capped columns with short trunk prepared at 160 ℃ (a,b) and ones with elongated trunk obtained at 150 ℃ (c–g). The high magnification HRTEM images of the four corners (d–g) of a single capped column nanocrystal (c) prepared at 150 ℃, confirmed that these capped columns with elongated trunk were single-crystalline.

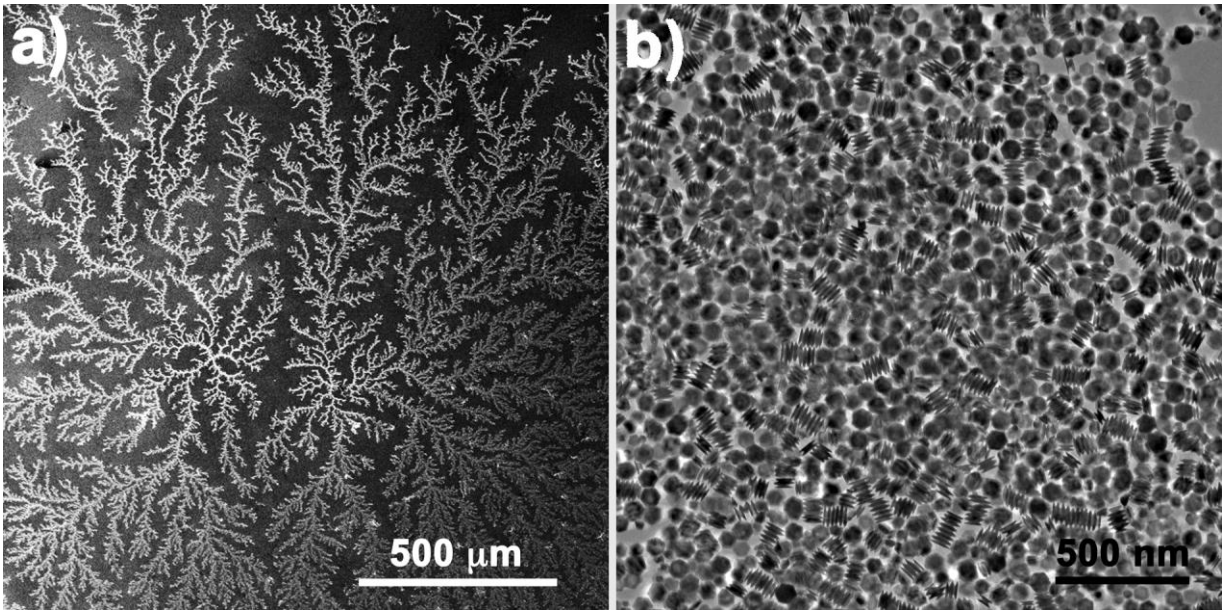

Figure S5. SEM (a) and TEM (b) images of the self-assembled Ru capped columns in large areas.

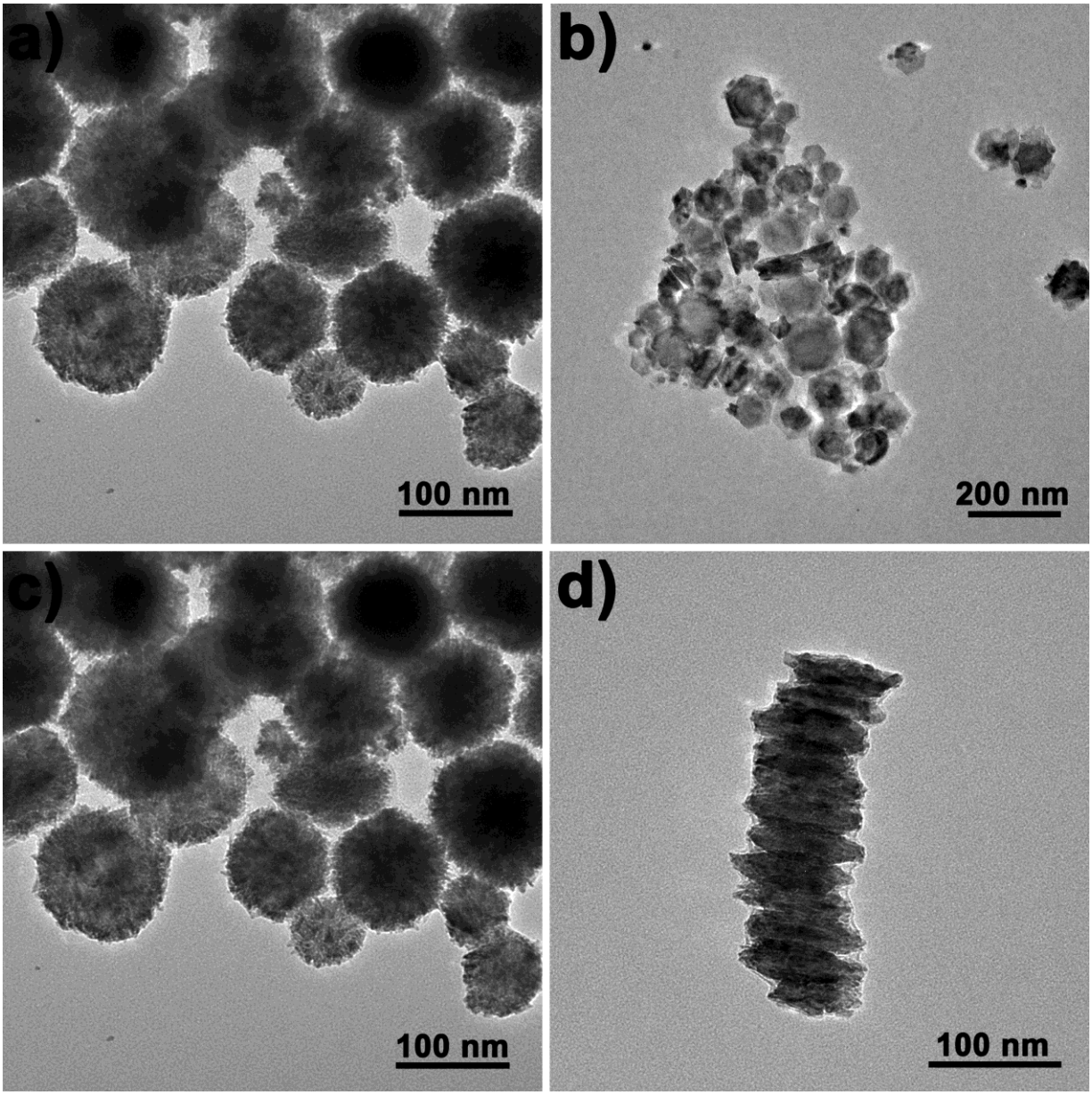

Figure S6. TEM images of Ru nanocrystals obtained with different molar ratios of Ru precursor to sodium oxalate (a-d): (a) 1 : 3; (b) 1 : 4; (c) 1 : 6; (d) 1 : 7.

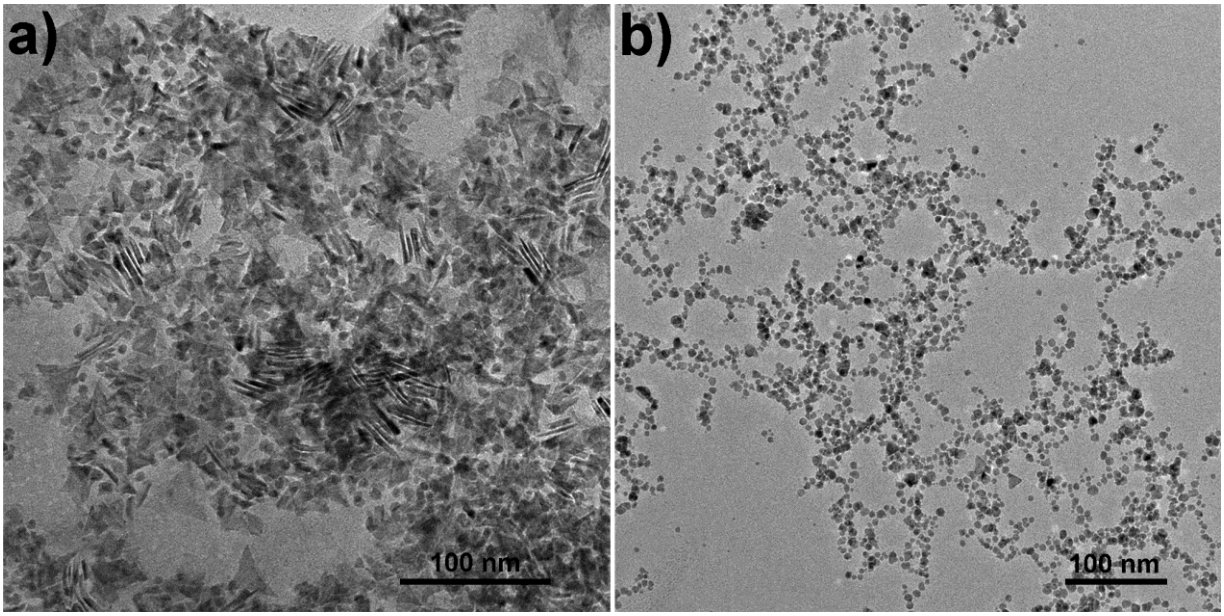

Figure S7. TEM images of Ru nanocrystals obtained under the following conditions: (a) without addition of $Na_2C_2O_4$, 0.12 mmol $RuCl_3$, 160 °C, 8 h; (b) 0.06 mmol $RuCl_3$, 80 mg of $Na_2C_2O_4$, 160 °C, 8 h.

Figure S8. Digital images of the reaction solution for the synthesis of Ru capped column nanocrystals after hydrothermal treatment at 160 ℃ for different reaction times (0–8 h). The "0 h" sample was the mixture of reagents initially added. Greenish yellow solutions were formed during the first 4 hours of the synthesis, and deep grey to black dispersions were obtained after 5 h of reaction.

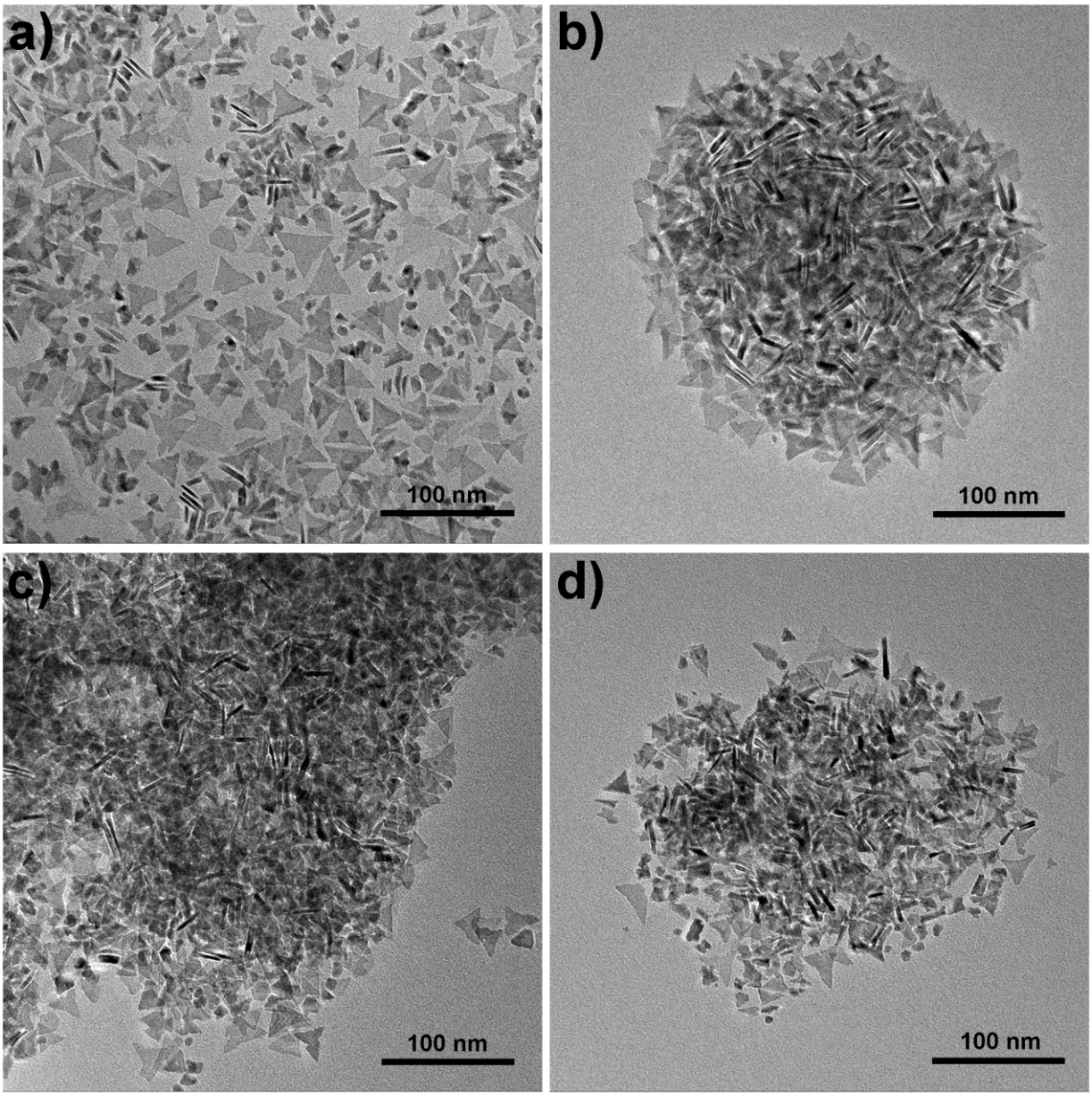

Figure S9. TEM images of Ru triangle nanoplates obtained with (a, b) different amounts of PVP (a: 50 mg, b: 200 mg) and (c, d) PVP molecules with different molecular weights (c: Mw = 10,000, d: Mw = 55,000).

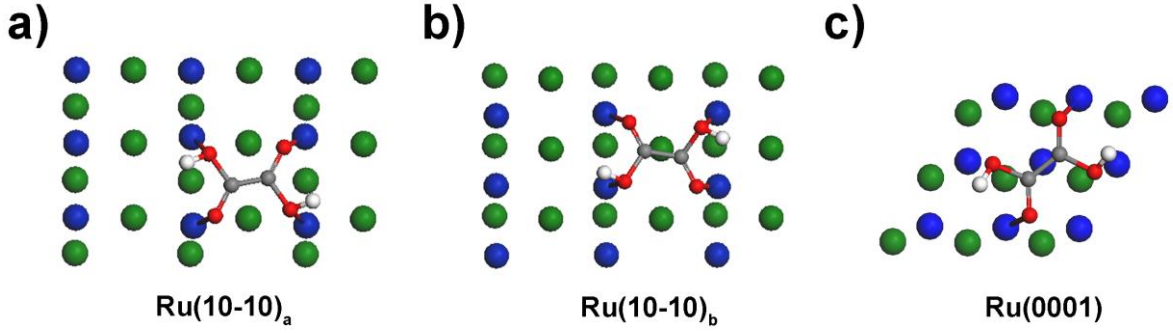

Figure S10. Top views of the adsorption geometries of oxalate species on $Ru(10\text{-}10)_a$ (a), $Ru(10\text{-}10)_b$ (b) and Ru(0001) (c). Big blue balls represent Ru atoms on the uppermost layer on certain facets, while big green balls represent inner Ru atoms. Small grey, red and white balls represent C, O, H atoms, respectively.

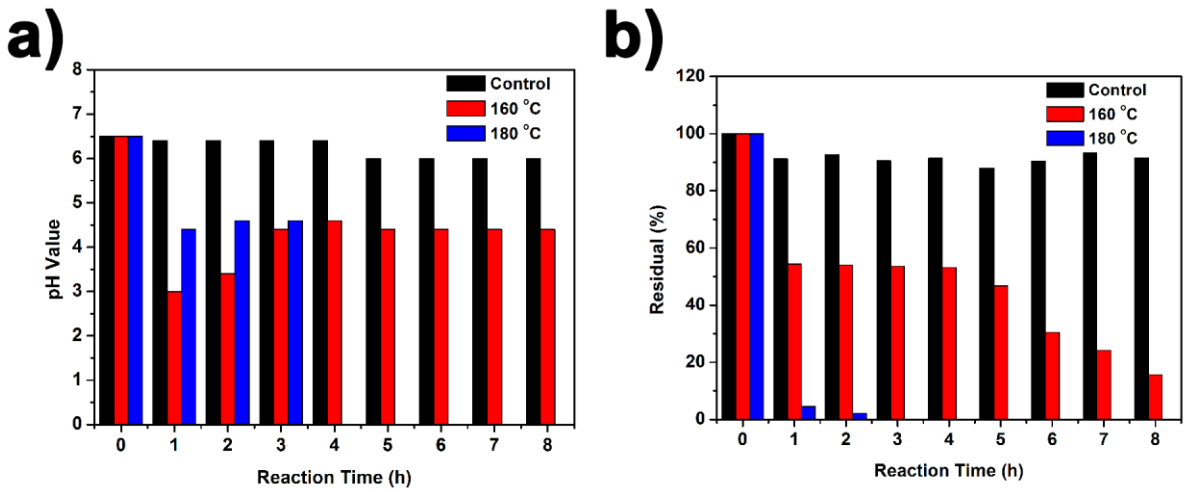

Figure S11. Variations of the pH values and the residual oxalate concentrations (as determined by the conventional titration method with $KMnO_4$ solution as the oxidant) of the reaction solutions in time-sequential experiments at 160 and 180 °C, respectively. In the "control" experiment, in which no other reagents but only proper amount of sodium oxalates aqueous solution was added, the pH values and residual concentrations of sodium oxalates changed slightly, indicating the high stability of oxalates under neutral conditions. The decrease of pH values of the reaction solutions should be the result of oxidation of HCHO by Ru(III) species at the beginning of the reaction (the oxidation of HCHO should generate CO_x and H^+). After that, the generated H^+ cations in the reaction solution would accelerate the thermal decomposition of oxalates (oxalic acid, which is unstable at high temperatures) and lead to the increase of pH values of the reaction solution. The concentration of residual oxalates determined by titration were referred to the free oxalates in solution before 5 h and the decomposition of the total oxalate species in the first 5 h could be illustrated by the decrease of extinction peak of ruthenium oxalates as shown in Figure 7.

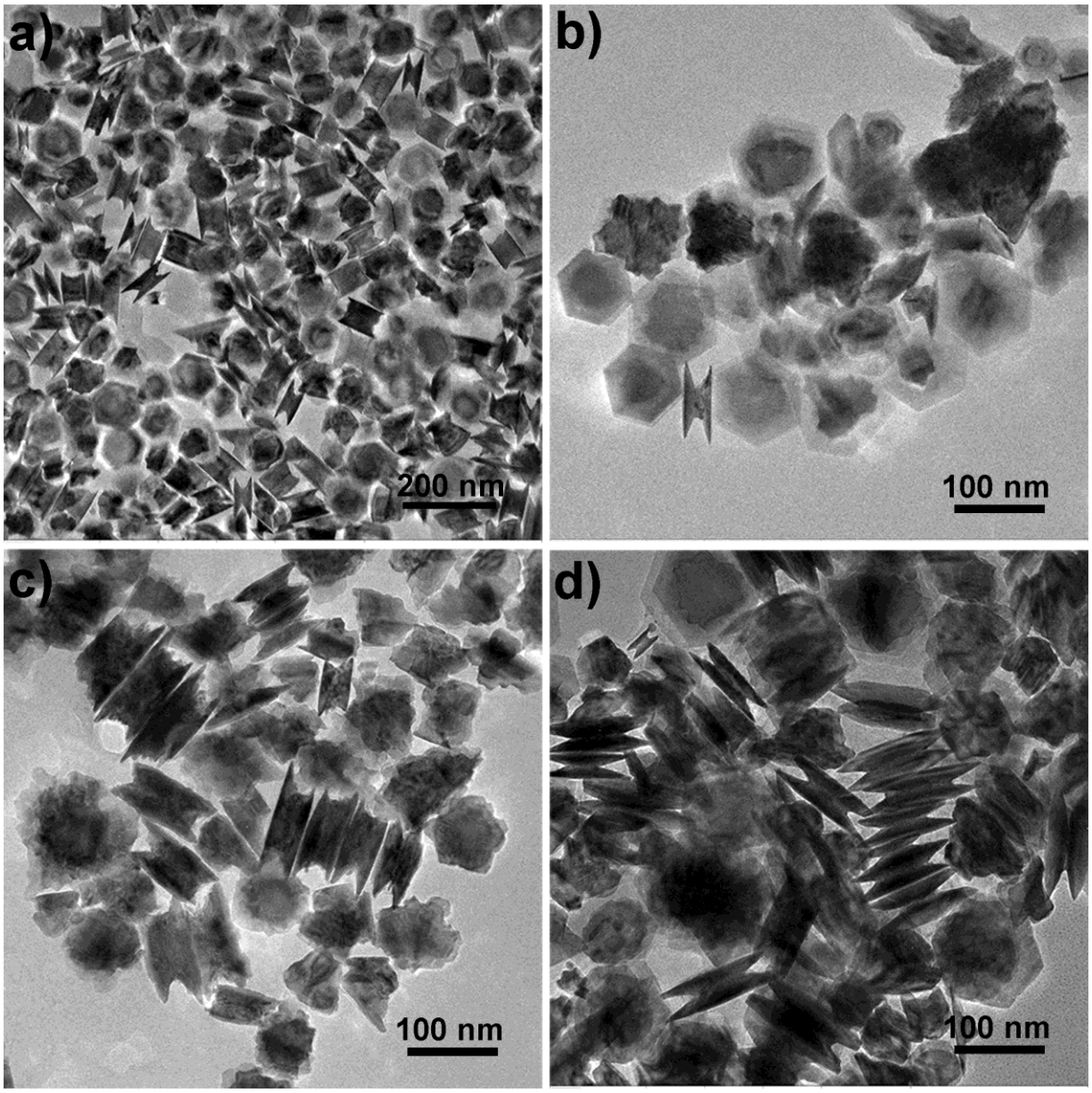

Figure S12. TEM images of Ru capped columns obtained with (a, b) different amounts of PVP (a: 50 mg, b: 200 mg) and (c, d) PVP molecules with different molecular weights (c: Mw = 10,000, d: Mw = 55,000).

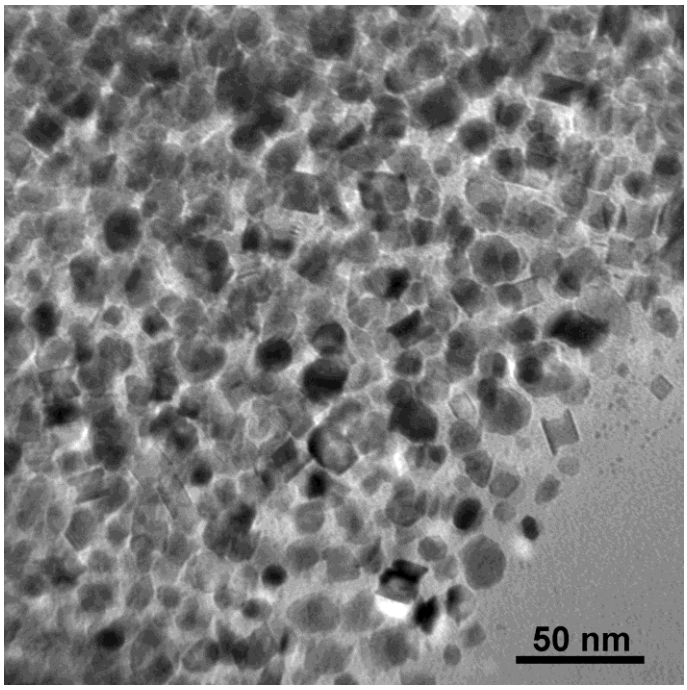

Figure S13. TEM image of Ru nanocrystals taken at the reaction time of 12 h under the otherwise conditions at 150 ℃ for a 24 h reaction, which shows the formation of barely capped column-like nanostructures as the intermediates during the shape evolution process of the capped columns.

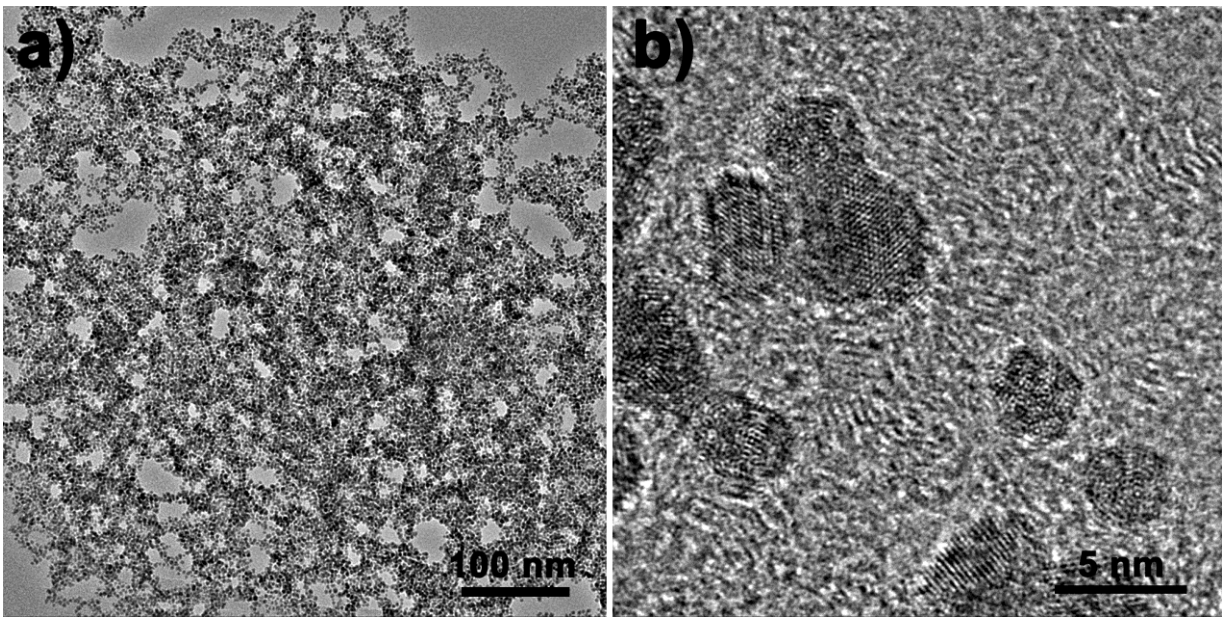

Figure S14. TEM (a) and HRTEM (b) images of the Ru nanospheres.

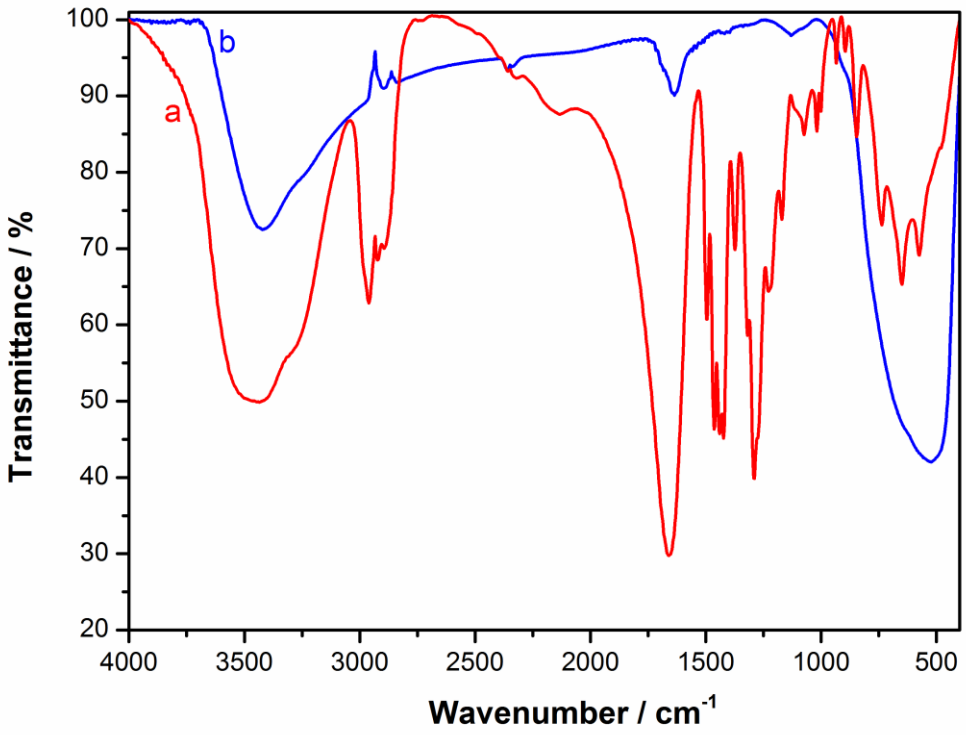

Figure S15. IR spectra (obtained on Bruker Vector22 FTIR spectrometer) of pure PVP (Mw = 29,000) (a) and the Ru/TiO_2 nanocatalyst after the catalytic measurement (b). In this figure, the appearance of the vibration peak of C=O at 1636 cm^{-1} for the nanocatalyst indicated the existence of trace amount of PVP on the surfaces of loaded Ru nanocrystals. The observation of a red shift of ca. 25 cm^{-1} in the vibration peak of C=O for the Ru nanocatalyst as compared with that of pure PVP was attributed to the coordination of PVP molecules with Ru nanocrystals by their O atoms (Ref. S2). Previously, PVP coated on the surfaces of metal nanoparticles was demonstrated to decompose at relatively high temperature of ca. 359 ℃ (see Ref. S3). In our case, such a high temperature might destruct the shapes of Ru nanoplates and capped columns via melting. Therefore, trace amount of PVP was allowed to present on the surfaces of the Ru nanocatalysts without severely affecting the shape dependent catalytic properties for our shape-controlled Ru samples. Similar cases have been demonstrated by some previous works on the catalytic measurements of PVP capped metal nanocrystals with controllable shapes such as Pt (Ref. S4) and Rh (Ref. S5) nanocubes in thermal heterogeneous reactions.

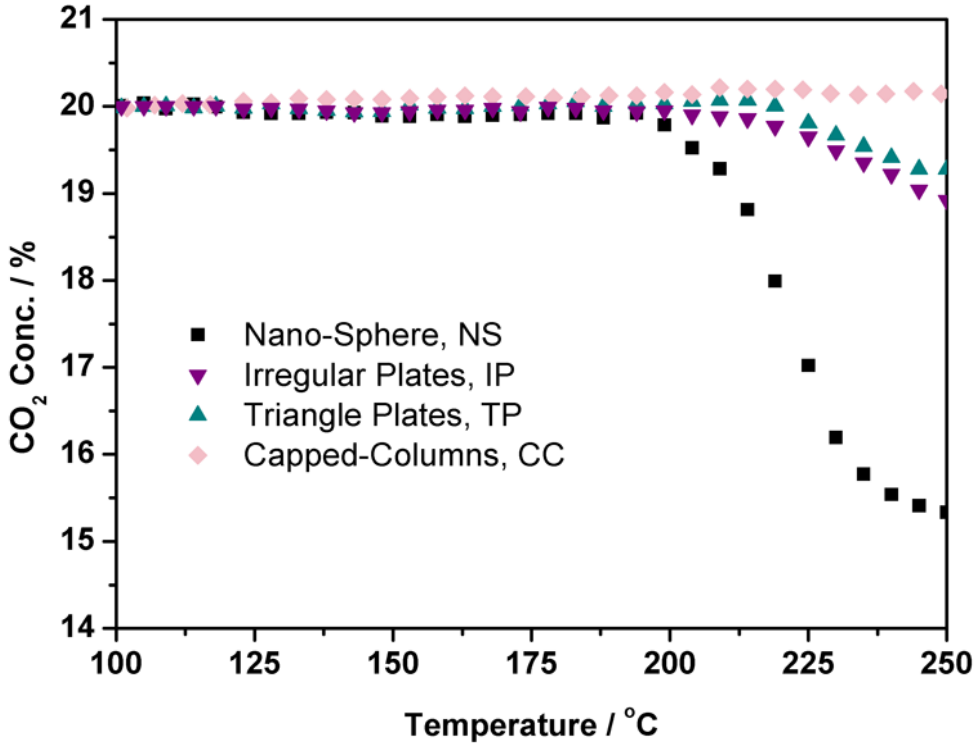

Figure S16. Temperature dependence of CO_2 outlet concentrations over Ru nanocrystals (1 wt% on TiO_2) with the shape of nanospheres (NS), irregular plates (IP), triangle plates (TP), and capped columns (CC), for the CO selective methanation reaction.

Ref. S1 Haglund, J.; Fernandez Guillermet, A.; Grimvall, G.; Korling, M. *Phys. Rev. B* **1993**, *48*, 11685.

Ref. S2 Wang, H. S.; Qiao, X. l.; Chen, J. G.; Wang, X. J.; Ding, S. Y. *Mater. Chem. Phys.* **2005,** *94*, 449.

Ref. S3 (a) Kim, C.; Min, M.; Chang, Y. W.; Yoo, K. - H.; Lee, H. *J. Nanosci. Nanotechnol.* **2010**, *10*, 233. (b) Shen, J.; Yin, X.; Karpuzovb, D.; Semagina, N. *Catal. Sci. Technol.* **2012,** doi: 10.1039/C2CY20443F.

Ref. S4 Tsung, C. K.; Kuhn, J. N.; Huang, W. Y.; Aliaga, C.; Hung, L. I.; Somorjai, G. A.; Yang, P. D. *J. Am. Chem. Soc.* **2009**, *131*, 5816.

Ref. S5 Zhang, Y. W.; Grass, M. E.; Kuhn, J. N.; Tao, F.; Habas, S. E.; Huang, W. Y.; Yang, P. D.; Somorjai, G. A. *J. Am. Chem. Soc.* **2008**, *130*, 5868.